Contemporary Clinical Trials Communications 38 (2024) 101260

Contents lists available at ScienceDirect

Contemporary Clinical Trials Communications

journal homepage: www.elsevier.com/locate/conctc

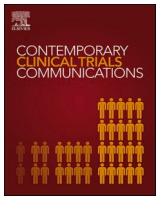

Optimal lesion preparation before implantation of a Magmaris bioresorbable scaffold in patients with coronary artery stenosis: Rationale, design and methodology of the OPTIMIS study

Kirstine Nørregaard Hansen [a,b,*], Akiko Maehara [c], Manijeh Noori [a,b], Jens Trøan [a], Christian Oliver Fallesen [a], Mikkel Hougaard [a], Julia Ellert-Gregersen [a], Karsten Tange Veien [a], Anders Junker [a], Henrik Steen Hansen [a,b], Jens Flensted Lassen [a,b], Lisette Okkels Jensen [a,b]

[a] Department of Cardiology, Odense University Hospital, Odense, Denmark
[b] University of Southern Denmark, Odense, Denmark
[c] Cardiovascular Research Foundation, New York Presbyterian Hospital, New York, USA

ARTICLE INFO

Keywords:
Intravascular imaging
Bioresorbable scaffolds
Optical coherence tomography
Intravascular ultrasound

ABSTRACT

Introduction: Percutaneous coronary intervention with implantation of a bioresorbable scaffold (BRS) provide the vessel support for a limited period allowing the vessel to restore normal vasomotion after degradation of the BRS, opposed to treatment with drug-eluting stents where the metal persist in the vessel wall. Late lumen loss and reduction in lumen area after implantation have been reported. The purpose of this study was to investigate whether intense pre-dilatation before BRS implantation resulted in less reduction of minimal lumen area at 6- and 12-month follow-up after implantation of a Magmaris BRS (MgBRS). Coronary imaging with optical coherence tomography (OCT) and intravascular ultrasound (IVUS) was assessed to track changes in lumen and vessel dimensions.

Methods: The prospective Optimal lesion PreparaTion before Implantation of the Magmaris bioresorbable scaffold In patients with coronary artery Stenosis (OPTIMIS) study randomly assigned eighty-two patients with chronic coronary syndrome to two pre-dilatation treatment strategies. Patients were randomized in a 1:1 ratio to pre-dilatation with either a non-compliant scoring balloon or a standard non-compliant balloon prior to implantation of a MgBRS. The treated segment was evaluated with OCT and IVUS at baseline, after 6 and 12 months to assess changes in lumen and vessel dimensions. The hypothesis was that more intense pre-dilatation with a non-compliant scoring balloon before MgBRS implantation can reduce the risk of late lumen reduction compared to standard pre-dilatation. The power calculation used expected MLA after 6 months (6.22 mm^2 for the scoring balloon and 5.01 mm^2 for the standard non-compliant balloon), power of 80 %, significance level of 0.05 and expected drop-out rate of 15 %, requiring 82 patients to be enrolled.

Results: Eighty-two patients were included in the study. Enrollment was from December 2020 to September 2023.

Conclusion: The hypothesis was that more intense pre-dilatation with a non-compliant scoring balloon before MgBRS implantation can reduce the risk of late lumen reduction compared to standard pre-dilatation.

1. Introduction

The treatment of coronary artery stenosis with percutaneous coronary intervention (PCI) has continued to improve throughout the years [1]. Bioresorbable scaffolds (BRS) have been developed to overcome safety and efficacy issues of bare-metal stents (BMS) and drug-eluting stents (DES) [2], such as late stent thrombosis. Implantation of a BRS in a coronary artery lesion provides the vessel support for a limited period allowing the vessel to obtain its original function and flexibility after the BRS has vanished [3,4]. Previous studies have shown that coronary lesions treated with early generation Magmaris BRS (Biotronik AG, Bülach, Switzerland) (MgBRS) resulted in lumen area reduction within the first year after implantation [5–7]. The exact mechanism is unclear, but increased plaque burden compromising the scaffold area,

* Corresponding author. Odense University Hospital, Department of Cardiology, Sdr. Boulevard 29, 5000, Odense C, Denmark.
E-mail address: kirstine.norregaard.hansen@rsyd.dk (K.N. Hansen).

https://doi.org/10.1016/j.conctc.2024.101260
Received 11 October 2023; Received in revised form 2 January 2024; Accepted 15 January 2024
Available online 7 February 2024

increased neointimal formation in the early phase of vascular healing, fast BRS resolution or constrictive remodeling have been considered as contributing factors [8,9]. Due to lower radial strength of the BRS compared to metal stents [10], repeat post-dilatation after implantation should be avoided, because of increased risk of dismantling causing BRS collapse and recoil. Instead, plaque modification with more intense lesion preparation prior to BRS implantation may be necessary to obtain optimal result [9,11].

The vascular healing and resorption of the BRS have been evaluated with intravascular ultrasound (IVUS) and optical coherence tomography (OCT) [12–14]. OCT provides detailed information about neointimal coverage, scaffold apposition, and vascular healing on microscopic level emphasizing luminal structures, while IVUS with its deeper tissue penetration provides better information on the abluminal level enabling assessment of vessel remodeling [14]. Conventional stent evaluation with intravascular imaging is based on visible struts and includes in-scaffold parameters such as scaffold area, strut coverage, and incomplete strut apposition. Metallic struts appear as reflective structures causing a shadow cast behind it in OCT assessment. However, degradation of the BRS over time makes conventional stent analysis less feasible as the majority of struts are often vanished at follow-up [15]. In previous BRS studies, OCT has been used to investigate the vascular healing of the BRS, but optimal consensus is not yet obtained [6,7,16–20].

The hypothesis of the Optimal lesion PreparaTion before Implantation of the Magmaris bioresorbable scaffold In patients with coronary artery Stenosis (OPTIMIS study) was that intensive lesion preparation and pre-dilatation with a scoring balloon prior to implantation of a MgBRS may reduce lumen area reduction at 6 months follow-up compared to a standard lesion preparation with a non-compliant balloon.

2. Methods

2.1. Study design

The study was a prospective, single-centered, open-label randomized trial conducted at Odense University Hospital, Denmark comparing intense lesion preparation and pre-dilatation with a scoring balloon to lesions preparation with a standard non-compliant balloon, prior to implantation of a MgBRS. Enrollment was from December 2020 to September 2023. The patients were randomly allocated to the two treatment methods in a 1:1 ratio (Fig. 1). The physician analyzing the offline images was to the pre-dilatation method.

2.2. Ethics

The study was approved by the Regional Committees on Health Research Ethics for Southern Denmark (Project-ID: S-20200114) and Danish Data Agency (Journal no.: 20/49900), and was registered with ClinicalTrials.gov (NCT04666584).

All patients provided written informed consent for trial participation before randomization. A physician informed all patients before the baseline procedure about the procedure, potential complications and possibility of trial participation. A written patient information form in Danish was given to the patients prior to the procedure, and they were given a consideration period before inclusion. The patients gave written consent to a physician to participate in the OPTIMIS trial including clinical follow-up and angiography with IVUS and OCT after 6 months. All patients were informed of their right to withdrawn consent if wanted.

2.3. Patient population

Patients with chronic coronary syndrome were eligible, if they met inclusion and exclusion criteria (Table 1). Patients were screened for protocol inclusion and exclusion criteria before enrolment. Enrolled patients underwent clinical and invasive imaging follow-up with OCT and IVUS after 6 months, and the first 41 enrolled patients underwent additional invasive imaging follow-up after 12 months. Clinical and procedural characteristic are presented in Table 2.

2.4. Device

The MgBRS (Biotronik AG, Bülach, Switzerland) is a CE-marked metallic based BRS based on a magnesium alloy and coated with bioresorbable poly-L-lactic acid carrying the eluted drug sirolimus. The antiproliferative drug is applied to the scaffold at a dose of approximately 1.4 μg per mm^2 scaffold and is released completely after 100 days. The BRS is designed with 6 peaks and valleys forming an in-phase sinusoidal ring, linked with 2 slopes of connectors. The strut thickness is 150 μm. The magnesium alloy is first absorbed when it reacts to water creating magnesium-hydroxide which slowly transforms to amorphous

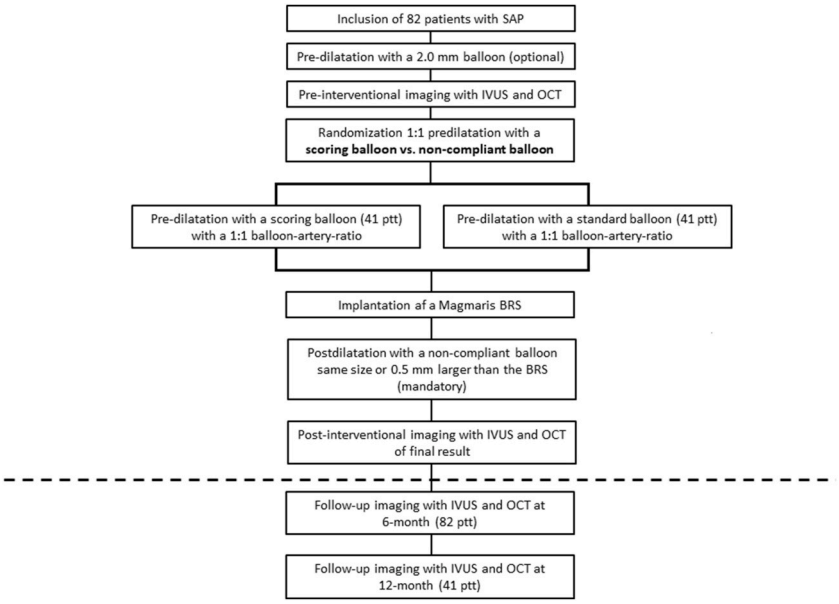

Fig. 1. Flow-chart.

Table 1
Inclusion and exclusion criteria.

Inclusion criteria	Exclusion criteria
Patients with chronic coronary syndrome scheduled for PCI in a native coronary artery	Ostial lesions (cannot be cleared with flushed contrast by OCT)
Age ≥18 years and ≤80 years	Significantly calcified lesions defined with an arc >180° and calcium thickness >0.5 mm and calcium length of >5 mm evaluated with IVUS and/or OCT).
Lesions treatable with a 3.0 or 3.5 mm Magmaris scaffold (coronary artery diameter between ≥2.75 mm and ≤4.0 mm)	Lesions longer than 40 mm Tortuous coronary arteries where the PCI-operator estimated that the introduction of an OCT-catheter would not be possible or would be associated with increased risk Allergy to aspirin, ticagrelor, clopidogrel, prasugrel or sirolimus eGFR <30 ml/min or creatinine >150 μg/L (due to the required amount of contrast by OCT) Expected survival <1 year Patients participating in other randomized stent studies

Abbreviations: IVUS; IntraVascular UltraSound OCT = Optical Coherence Tomography; PCI = Percutaneous Coronary Intervention.

Table 2
Patient baseline characteristics.

	Scoring balloon N = 41	Standard balloon N = 41
Age, years	64.9 ± 8.95	64.8 ± 7.89
Male, n (%)	27 (65.9)	28 (68.3)
Family history of IHD, n (%)	19 (46.3)	17 (41.5)
History of smoking, n (%)		
Current smoker	6 (14.6)	6 (14.6)
Previous smoker	21 (51.2)	11 (26.8)
Hypertension, n (%)	17 (41.5)	25 (61.0)
Hypercholesterolemia, n (%)	11 (26.8)	13 (31.7)
Diabetes mellitus, n (%)	4 (9.8)	8 (19.5)
BMI. mean (SD). kg/m^2	27.9 ± 9.7	27.9 ± 3.7
eGFR, ml/min	79.7 ± 12.5	82.1 ± 11.6
Creatinin, μmol/L	79.8 ± 17.2	77.7 ± 15.2
Previous MI, n (%)	9 (22.0)	4 (9.8)
Previous PCI, n (%)	11 (26.8)	6 (14.6)
Previous CABG, n (%)	0 (0.0)	0 (0.0)
Treated coronary artery, n (%)		
Left anterior descending	23 (56.1)	24 (58.5)
Left circumflex	6 (14.6)	8 (19.5)
Right coronary artery	12 (29.3)	9 (22.0)

Baseline characteristics did not differ significantly among the two groups.

calcium phosphate with high water content. The MgBRS is completely absorbed after 1 year [21]. The scaffold are available in sizes with a diameter of 3.0 mm and 3.5 mm, and lengths of 15, 20 and 25 mm.

The ScoreFlex non-compliante scoring angioplasty catheter (Orbus-Neich Medical Trading, Inc., Fort Lauderdale, FL) is a mono-rail type scoring balloon with an integral nitinol wire fixed around the balloon acting as scoring element, when the balloon is inflated. The dual-wire semi-compliant balloon system allows focused force dilatation and safe and controlled plaque modification. The ScoreFlex balloon is available in diameters spanning from 1.75 to 4.0 mm and lengths of 10–20 mm [22].

2.5. Procedure strategy

The procedural method is illustrated in Fig. 1. Study lesions were treated with a MgBRS in all patients. Patients received a dose of heparin (70 UI/kg) prior to the PCI procedure. The coronary stenosis was identified by the PCI operator's interpretation of the angiographic findings. Imaging with OCT and IVUS was performed to evaluate vessel size, length and plaque morphology of the lesion to assure that the lesion was treatable with a MgBRS. Pre-dilatation with a 2.0 mm balloon was allowed if necessary. The scaffold size was based on IVUS measurements of the proximal and distal reference external elastic membrane (EEM) diameters. If the EEM was visible in >180° of the CSA, the smaller EEM rounded down to the nearest 0.25 mm was used to determine scaffold diameter. If the EEM was visible in <180°, the scaffold diameter was based on the lumen diameter [23]. Patients were randomized 1:1 to either 1) lesion preparation with a scoring balloon, or 2) standard pre-dilatation with a non-compliant balloon. The lesion was predilated with the randomized treatment technique in a 1:1 balloon-artery ratio with a residual stenosis of less than 20 %. If the pre-dilatation goal was not achieved, up-scaling to a 0.5 mm larger scoring balloon was allowed in the study arm randomized to treatment with a scoring balloon. In the standard treatment study arm, upscaling to a 0.5 mm larger non-compliant balloon was allowed.

After lesion preparation, a MgBRS was implanted. Inflation pressure at scaffold implantation was maintained for 25–30 s. Post-dilatation was perfomed with a non-compliant balloon the same size as the scaffold or maximally 0.5 mm larger than the scaffold applying nominal pressure. Finally, OCT- and IVUS images were acquired and controlled by the PCI-operator and an on-site dedicated OCT-analyst. Additional post-dilatation with a non-compliant balloon was only allowed if there was major under-expansion (defined as MSA <4.5 mm^2) or major malapposition (defined as strut >0.3 μm from the lumen wall for >3 mm) assessed with OCT. Additional scaffolding was allowed in the presence of significant edge dissection or residual stenosis <5 mm proximal or distal to the scaffold (causing MLA <4 mm^2). OCT and IVUS images of the final result were obtained. Follow-up OCT and IVUS were performed after 6 and 12 months. Patient characteristics are presented in Table 2.

2.6. Intravascular imaging and analysis

2.6.1. Optical coherence tomography

OCT will be performed at baseline, at 6-month follow-up for all patients and 12-month follow-up for the first 41 enrolled patients. The imaging procedures will be preceded by administration of 200 μg of intracoronary nitroglycerin. OCT will be performed with frequency-domain OPTIS OCT system (Illumien OCT system; Abbott Vascular, Santa Clara, CA) and the Dragonfly™ Imaging catheter. The catheter will be placed approximately 10 mm distally to the lesion. The coronary artery is flushed with 15 ml contrast injection to clear the coronary artery of blood for optimal imaging quality during automated pullback at a rate of 20 mm/s over a distance of 70 mm. An independent imaging-analyst blinded to the pre-dilatation technique will use the OCT off-line software (Offline Review Workstation; St. Jude) for quantitative OCT analysis. The analysis of the scaffold-treated segment will be analyzed at cross section area (CSA) level with a distance of 1 mm (every 5 frames).

2.6.2. Intravascular ultrasound

Intravascular imaging with IVUS will be performed at baseline before and after stenting, and after 6-month for all patients and after 12-month follow-up for the first 41 of the patients. The OptiCross 2.6 Fr IVUS-catheter will be positioned at least 10 mm distally to the lesion or stented segment. Imaging acquisition using motorized IVUS pullbacks will be performed with pullback speed of 0.5 mm/s after intracoronary bolus of 200 μg nitroglycerine at 40 MHz (Boston Scientific, Marlborough, MA, USA). The baseline IVUS pullbacks will be matched with the follow-up IVUS imaging using anatomical landmarks. IVUS pullbacks will be analyzed by an independent analysist blinded to pre-dilatation method with the commercially available program for computerized analysis (Echoplaque, INDEC Systems, Inc., Santa Clara, CA, USA). The IVUS measurements will be analyzed at a cross-sectional level at baseline and follow-up, and are calculated every 1 mm within the scaffold-treated segment.

3. OCT and IVUS measurements

OCT imaging measurements include lumen dimensions available at baseline and follow-up: MLA, mean lumen area (LA), lumen volume, and change in MLA (baseline MLA – follow-up MLA) in the scaffold-treated segment. Scaffold dimensions include minimal scaffold area (MSA), mean scaffold area (SA), minimum scaffold diameter (MSD), scaffold volume, number of struts at baseline and strut remnants at follow-up, and scaffold expansion (MSD/manufacturer's compliance chart-predicted MSD). Quantitative analysis on scaffold level is limited to baseline images to some extent due to fast absorption of the scaffold, which makes the detection of struts difficult at follow-up. Incomplete scaffold apposition is defined as malapposed when the distance between the abluminal surface of the strut and the luminal surface of the vessel wall exceeds the struts thickness of 150 μm. At baseline, malapposition area, distance and volume will be analyzed. At follow-up, visible struts or strut remnant will be categorized as malapposed when the abluminal border of the strut/remnant is separated from the lumen surface by a visible space exceeding 150 μm. The malapposition observations will be matched from baseline to follow-up and will be divided into acute/late, resolved, persistent or acquired malapposition. OCT images of the MgBRS at baseline and follow-up is represented in Fig. 2.

IVUS imaging measurements include lumen and scaffold dimensions as described above. Quantitative analysis includes measurements of external elastic membrane (EEM), peri-scaffold plaque (EEM area – SA), scaffold-edge plaque (EEM area – LA), total plaque area (EEM area – LA), remodeling index (RI) (lesion EEM CSA/(EEM CSA proximal + EEM CSA distal reference)/2) and change in RI (RI at follow-up – RI at baseline). Serial evaluation of remodeling will be performed. The EEM at MLA in the lesion before treatment will be measured and matched to the comparable cross section site post-procedure and at follow-up. The change in EEM from baseline to follow-up will determine the change in remodeling over time. Negative remodeling is defined as a decrease in EEM area over time, and positive remodeling is defined as enlargement of the EEM area. Serial comparison between OCT and IVUS in a MgMRS treated artery is represented in Fig. 3.

3.1. Primary endpoint

The primary endpoint is MLA in the scaffold-treated segment after 6 months assessed with OCT.

3.2. Secondary endpoint

The secondary endpoints are change in MLA from baseline to follow-up after 6 and 12 months, serial change in RI, and percentage of incomplete scaffold apposition.

3.3. Statistical analysis

Assuming data are normally distributed, categorical data will be presented as numbers and frequencies and compared using chi2-test. Continuous data will be presented as mean ± SD and compared using Student t-test. For variables not normally distributed non-parametric testing with Mann-Whitney *U* test will be performed, and the median and interquartile ranges will be reported. SPSS version 26.0 will be used for the statistical analysis. The estimated sample size is based on data, from the Coronary Artery Healing Process after Optical Coherence Tomography Guided Percutaneous Coronary Intervention with Magmaris Bioresorbable Scaffold in Patients with Non-ST-Segment-Elevation Myocardial Infarction (the HONEST study) [9]. In the HONEST study, all lesions were predilated with a standard non-compliant balloon prior to implantation of a MgBRS. MLA at 6-month follow-up was measured with OCT and showed a reduction from 6.99 mm^2 to 5.01 mm^2. The power analysis in the current study was also based on OCT measurement of MLA 6 month after implantation, and the results from the HONST study was used as our reference group. In the standard non-compliant balloon lesion preparation group, the expected reduction of MLA was 6.99 mm^2 to 5.01 mm (27 %) 6 months after implantation of the MgBRS. In the scoring balloon lesion preparation group, the expected reduction of MLA was 6.99 mm^2–6.22 mm^2 (11 %). A power calculation is conducted using the expected MLA after 6 months (6.22 mm^2 for the scoring balloon and 5.01 mm^2 for the standard non-compliant balloon). Inclusion of 35 patients in each group is necessary to reach statistical

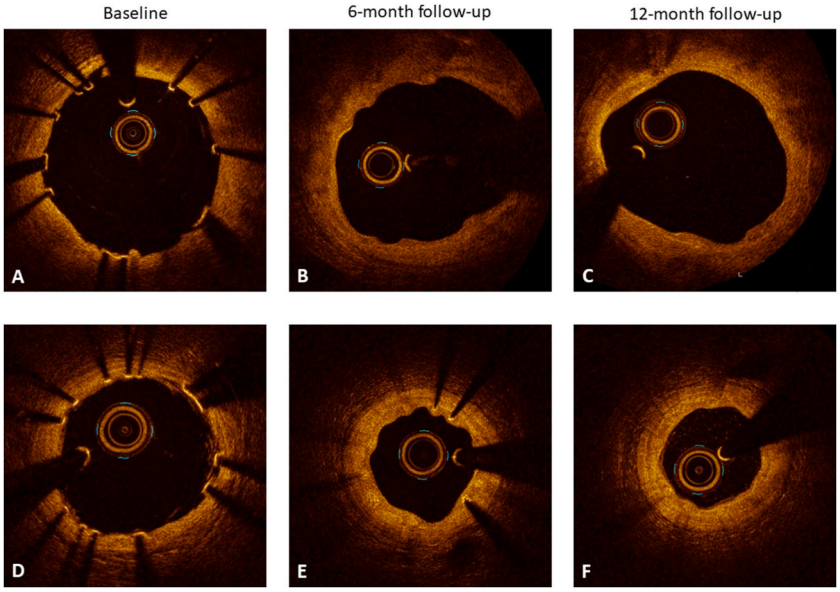

Fig. 2. Vascular healing after implantation of a Magmaris bioresorbable scaffold. Two serial OCT-images of vascular healing after implantation of a Magmaris bioresorbable scaffold. At baseline (A + D), analyzable struts are visible in the circumference of the vessel. Due to construction similarities between a metallic BRS and a drug-eluting stent, conventional analysis methodology is applicable to the Magmaris BRS at baseline. At follow-up, after 6-month (B + E) only few struts remnants are visible (B + E), and almost completely vanished after 12 month (C + F). At follow-up, the analysis is limited to in-segment measurements such as lumen dimensions. Favorable vascular healing is illustrated in the serial OCT-images (A–C) with unchanged lumen dimensions from baseline to 12-month follow-up, compared to poor vascular healing illustrated in the serial OCT images (D–F), where lumen area is reduced from baseline to follow-up.

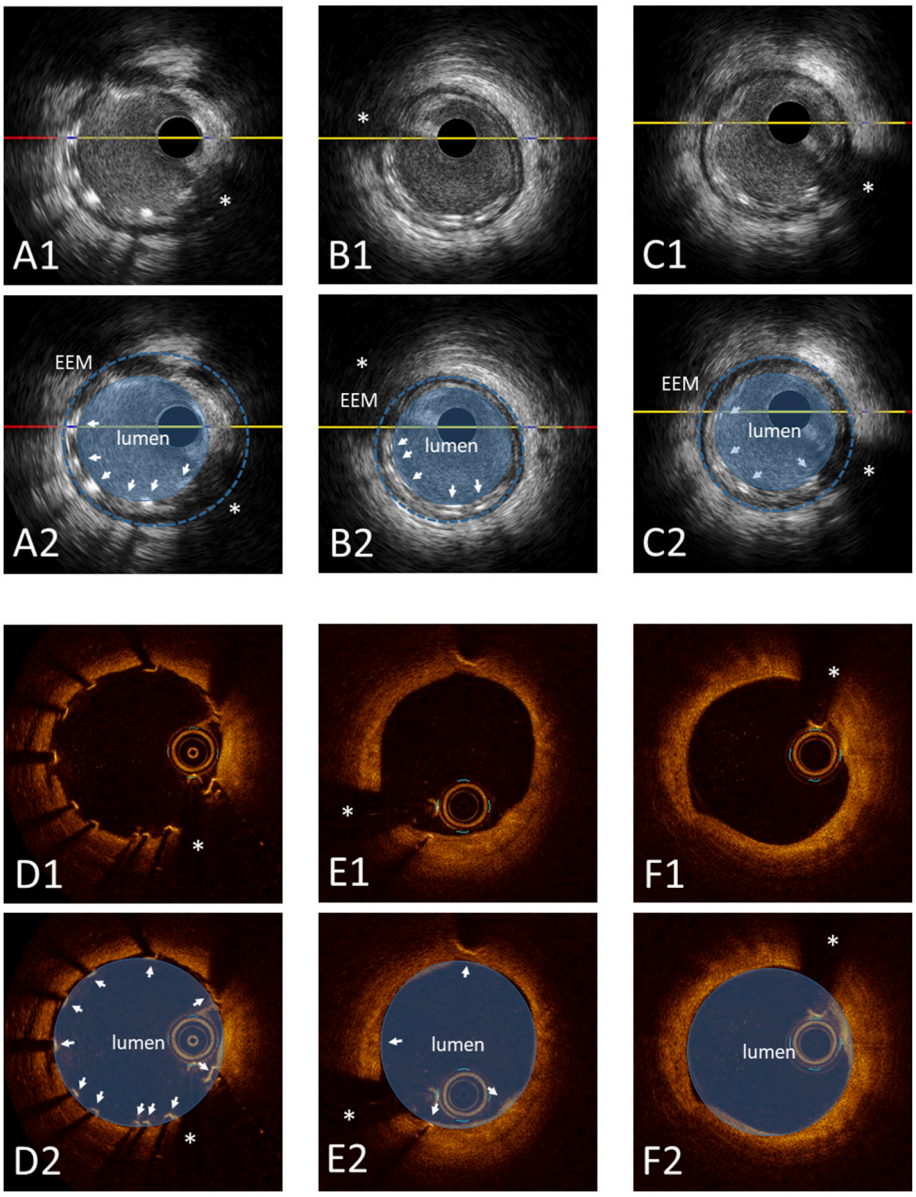

Fig. 3. Serial intravascular evaluation of the Magmaris bioresobable scaffold at baseline, 6- and 12-month follow-up. Serial intravascular evaluation at baseline (A + D), 6-month follow-up (B + E) and 12-month follow-up (C + F) with optical coherence tomography (OCT) (D–F) and intravascular ultrasound (IVUS) (A–C) after implantation of a Magmaris bioresobable scaffold (MgBRS). The cross sections are presented without (1) and with (2) analyzable measurements. Comparing IVUS (A–C) and OCT (D–F), lumen contours (solid line) are visible with both imaging modalities (A2-F2), but the external elastic membrane (EEM) (dashed line) is only detectable with IVUS (A2-C2). A1+A2 show the MgBRS treated segment at baseline, where scaffold struts (arrows) are visible at 5 to 10 o'clock. D1+D2 show the same segment with OCT. Scaffold struts are detectable (arrows) in the whole circumference of the artery. At 6-month follow-up (B + E), scaffold strut remnants (arrows) are detectable with both IVUS and OCT after 6-month. With IVUS (B), the remnants are still visible from 5 to 9 o'clock, but with OCT (E), the struts are partly dissolved and remnants are only analyzable at 5, 7, 9 and 12 o'clock. At 12-month follow-up (C + F), a part of scaffold remnants are still visible at 5, 7, 8 and 8 o'clock (C), but with OCT no struts seem to be discernible (F). Imaging catheter (*).

significance in case of 2-tailed significance level of 0.05 and power of 80 %. Loss to follow-up and poor image quality finalize an expected drop-out rate of 15 %, thereby requiring 82 patients in total.

4. Results

Enrollment was completed by September 8th' 2023. Baseline clinical characteristics are presented in Table 1. The treatment groups were well-matched without differences in baseline characteristics.

5. Discussion

The BRSs have been developed to provide temporary vessel support following PCI before degradation leaving the coronary artery to restore normal vasomotion and flexibility [3,4]. However, concerns about lumen reduction after implantation have been reported [7,9,16,18,24]. The aim of the study is to investigate whether a more intense lesion preparation with a scoring balloon compared to a standard non-compliant balloon will minimize lumen reduction after implantation of a MgBRS.

First-generation BRS (Absorb BRS, Abbott Vascular, Santa Clara, Ca) provided with an alternative approach to transient vascular support without permanent caging of the DES [25]. The Absorb BRS was composed of a poly-L-lactide polymer backbone and thicker struts to compensate for reduced radial strength compare to DES [24]. Even though promising functional testing showed sign of reestablishment of

normal vasomotion [26], an increased event rate of especially very late scaffold thrombosis was observed over time [27,28]. Other available biodegradable polymer scaffolds, such as the DESolve BRS (Elixir Medical Corp., Sunnyvale, USA) and the Fantom BRS (REVA medical, San Diego, USA) have longer absorption time of up to 2 and 4 years, respectively. Lumen reduction has been observed in both BRS after 6-months, but long-term imaging follow-up is not available [16,18]. Compared to biodegradable polymer scaffolds, the second-generation metallic BRS such as the MgBRS is made of a magnesium alloy and expected to have a higher radial strength but shorter absorption time compared to other BRS [29,30]. Even though long-term follow-up showed no scaffold thrombosis up to three years after implantation [5,31], observations of decrease in lumen area assessed with intravascular imaging over time [5,9,32,33] have raised questions about efficacy and concerns of higher restenosis rates compared to DES [6,7,9]. Due to lower radial strength of the MgBRS compared to DES, manipulation and repeated post-dilation after implantation may increase the risk of fracturing and dismantling of the BRS possibly leading to collapse and recoil [8,9]. It should be possible to avoid repeat post-dilatation after placement of the scaffold, if optimal lesion preparation is obtained. Register-based observational studies reported target-lesion revascularization (TLR) rate of 2.7–8.5 % after one year, and increasing up to 14 % after 5 years [34,35]. The prospective BIOSOLVE studies (BIOtroniks – Safety and performance in de nOvo Lesion of natiVE coronary arteries with Magmaris) including the largescale BIOSOLVE-IV trial showed low TLR rates of 1.6–3.9 % within one year in an all-comer population [36,37], and sustained efficacy after 5 years with a TLR rate of 5.9 % observed in a smaller population [38]. In contrast, the MAGSTEMI study (MAGnesium-based bioresorbable scaffold in ST-segment Elevation Myocardial Infarction) comparing a sirolimus-eluting stent to the MgBRS revealed TLR rate of 16.2 % within the first year [39] in patients presenting with STEMI with no difference between year 1 and 3 [40]. Several prospective studies have evaluated the change in lumen area with OCT or IVUS after implantation of the MgBRS, reporting reduction in lumen area over time [5–7,9,33,41]. Speculations of the mechanism behind scaffold restenosis and late scaffold recoil may be associated with negative remodeling, early scaffold absorption, premature loss in radial strength and impact of underlying plaque [8]. Optimal lesion preparation and pre-dilatation before implantation of the MgBRS may be crucial to overcome the issue of scaffold recoil. Vessel force and its effect on rapidly dissolving BRSs is until now uncertain, but vascular remodeling assessed with IVUS may help to clarify the mechanisms behind recoil and lumen reduction after implantation of the BRS.

In previous BRS studies, OCT has been used to investigate the vascular healing of the BRS, but optimal consensus has not yet been obtained [6,7,16–20]. Due to difference in degradation time, the measurable OCT parameters may differ among the BRS types. Table 3 shows an overview of four BRS types and the available intravascular measurements at baseline and 6-month follow-up. At 6-month, conventional analysis methodology is applicable for evaluation of Absorb BRS, Fantom BRS and DESolve BRS [16,24,42], but analysis requiring struts visibility – strut coverage, malapposition and scaffold dimensions – is not available at follow-up for analysis of the MgBRS due to a faster resorption [6,7,9] (Table 1). Therefore, the analysis at follow-up relies on lumen measurements and remodeling analysis alone.

Serial intravascular evaluation of the scaffold degradation over time show the need for a new technique to describe the healing process. Nakatani et al. [15] express the need for a different methodological approach when analyzing BRS compared to permanent stents and highlight that only flow area based on lumen contour is assessable at long-term follow-up. Other studies have invented new terminology with different healing states or stages to describe the OCT quantitative findings at follow-up [9,41,43] based on the discernibility of the remained struts. However, the quantitative OCT findings are usually limited to lumen measurements in the scaffold treated area. There is no clear consensus on how to report intravascular imaging analysis of BRSs at follow-up as scaffold struts may or may not be visible.

Table 3
Intravascular measurements available at baseline and 6-month follow-up for four bioresorbable scaffolds.

		Absorb	Desolve	Fantom	Magmaris
OCT	Baseline measurements				
	Lumen (area, diameter, volume)	x	x	x	x
	Vessel (area, diameter, volume)				
	Plaque (area, diameter, volume)				
	Scaffold (area, diameter, volume)	x	x	x	x
	Malapposition	x	x	x	x
	Strut coverage (percentage of uncovered struts, neointimal hyperplasia)	–	–	–	–
	Acute recoil (%)	x	x	x	x
	Follow-up measurements				
	Lumen (area, diameter, volume)	x	x	x	x
	Vessel (area, diameter, volume)				
	Plaque (area, diameter, volume)				
	Scaffold (area, diameter, volume)	x	x	x	
	Malapposition	(x)	(x)	(x)	
	Strut coverage (percentage of uncovered struts, neointimal hyperplasia)	(x)	(x)	(x)	
	Acute recoil (%)				
IVUS	Baseline measurements				
	Lumen (area, diameter, volume)	x	x	x	x
	Vessel (area, diameter, volume)	x	x	x	x
	Plaque (area, diameter, volume)	x	x	x	x
	Scaffold (area, diameter, volume)	x	x	x	x
	Malapposition	x	x	x	x
	Strut coverage (percentage of uncovered struts, neointimal hyperplasia)	–	–	–	–
	Acute recoil (%)	x	x	x	x
	Follow-up measurements				
	Lumen (area, diameter, volume)	x	x	x	x
	Vessel (area, diameter, volume)	x	x	x	x
	Plaque (area, diameter, volume)	x	x	x	x
	Scaffold (area, diameter, volume)	x	x	x	x
	Malapposition	x	x	x	(x)
	Strut coverage	x	x	x	(x)
	Acute recoil (%)				

Abbreviations: IVUS = intravascular ultrasound, NIH = Neointimal hyperplasia, OCT = optical coherence tomography.

The study had potential limitation. The primary endpoint was not clinically driven, but based on intravascular imaging findings, due to small sample size. The study was open-label, as the operator knew what kind of balloon was used for lesion preparation. Both the patients and the OCT and IVUS analysists were blinded to the type of balloon used for lesion preparation.

The OPTIMIS trial will focus on vessel reaction and the vascular mechanisms following the implantation of a MgBRS during the degradation up to 1 year after implantation. The study will investigate if intensive lesion preparation can optimize the treatment result and

minimize the lumen reduction over time.

Sources of funding

The study is an investigator-initiated trial, and did not receive any financial support.

CRediT authorship contribution statement

Kirstine Nørregaard Hansen: Writing – review & editing, Writing – original draft, Project administration, Methodology, Investigation, Formal analysis, Data curation, Conceptualization. **Akiko Maehara:** Writing – review & editing. **Manijeh Noori:** Writing – review & editing, Data curation. **Jens Trøan:** Writing – review & editing, Validation, Investigation, Data curation. **Christian Oliver Fallesen:** Writing – review & editing, Methodology, Conceptualization. **Mikkel Hougaard:** Writing – review & editing, Data curation. **Julia Ellert-Gregersen:** Writing – review & editing, Data curation. **Karsten Tange Veien:** Writing – review & editing, Data curation. **Anders Junker:** Writing – review & editing, Methodology, Investigation, Data curation, Conceptualization. **Henrik Steen Hansen:** Writing – review & editing, Investigation, Data curation, Conceptualization. **Jens Flensted Lassen:** Writing – review & editing, Methodology, Investigation, Data curation, Conceptualization. **Lisette Okkels Jensen:** Writing – review & editing, Supervision, Project administration, Methodology, Investigation, Data curation, Conceptualization.

Declaration of competing interest

The authors declare the following financial interests/personal relationships which may be considered as potential competing interests: KNH, MN, JT, COF, MH, KTV, JEG, AJ, AM, JFL, HSH have no conflict of interests. LOJ has received research grants from Biotronik, OrbusNeich, Biosensors, and Terumo to her institution; and honoraria from Biotronik.

Data availability

Data will be made available on request.

References

[1] R. Piccolo, K.H. Bonaa, O. Efthimiou, O. Varenne, A. Baldo, P. Urban, C. Kaiser, W. Remkes, L. Räber, A. de Belder, A.W.J. van 't Hof, G. Stankovic, P.A. Lemos, T. Wilsgaard, J. Reifart, A.E. Rodriguez, E.E. Ribeiro, P. Serruys, A. Abizaid, M. Sabaté, R.A. Byrne, J.M. de la Torre Hernandez, W. Wijns, P. Jüni, S. Windecker, M. Valgimigli, Drug-eluting or bare-metal stents for percutaneous coronary intervention: a systematic review and individual patient data meta-analysis of randomised clinical trials, Epub 2019/05/06, Lancet (London, England) 393 (10190) (2019) 2503–2510, https://doi.org/10.1016/s0140-6736(19)30474-x. PubMed PMID: 31056295.

[2] S. Bangalore, H.G. Bezerra, D.G. Rizik, E.J. Armstrong, B. Samuels, S.S. Naidu, C. L. Grines, M.T. Foster, J.W. Choi, B.D. Bertolet, A.P. Shah, R. Torguson, S.B. Avula, J.C. Wang, J.P. Zidar, A. Maksoud, A. Kalyanasundaram, S.J. Yakubov, B. M. Chehab, A.J. Spaedy, S.P. Potluri, R.P. Caputo, A. Kondur, R.F. Merritt, A. Kaki, R. Quesada, M.A. Parikh, C. Toma, F. Matar, J. DeGregorio, W. Nicholson, W. Batchelor, R. Gollapudi, E. Korngold, R. Sumar, G.S. Chrysant, J. Li, J. B. Gordon, R.M. Dave, G.F. Attizzani, T.P. Stys, O.S. Gigliotti, B.E. Murphy, S. G. Ellis, R. Waksman, The state of the Absorb bioresorbable scaffold: consensus from an expert panel, Epub 2017/12/09, JACC Cardiovasc. Interv. 10 (23) (2017) 2349–2359, https://doi.org/10.1016/j.jcin.2017.09.041. PubMed PMID: 29216997.

[3] R. Waksman, P. Zumstein, M. Pritsch, E. Wittchow, M. Haude, C. Lapointe-Corriveau, G. Leclerc, M. Joner, Second-generation magnesium scaffold Magmaris: device design and preclinical evaluation in a porcine coronary artery model, Epub 2017/03/07, EuroIntervention : J. EuroPCR Coll. Working Group Intervent. Cardiol. Europ. Soc. Cardiol. 13 (4) (2017) 440–449, https://doi.org/10.4244/eijd-16-00915. PubMed PMID: 28262623.

[4] Y. Zhang, C.V. Bourantas, V. Farooq, T. Muramatsu, R. Diletti, Y. Onuma, H. M. Garcia-Garcia, P.W. Serruys, Bioresorbable scaffolds in the treatment of coronary artery disease, Epub 2013/05/11, Med. Dev. (Auckland, NZ) 6 (2013) 37–48, https://doi.org/10.2147/mder.s22547. PubMed PMID: 23662091; PMCID: PMC3647349.

[5] M. Haude, R. Erbel, P. Erne, S. Verheye, H. Degen, D. Böse, P. Vermeersch, I. Wijnbergen, N. Weissman, F. Prati, R. Waksman, J. Koolen, Safety and performance of the drug-eluting absorbable metal scaffold (DREAMS) in patients with de-novo coronary lesions: 12 month results of the prospective, multicentre, first-in-man BIOSOLVE-I trial, Epub 2013/01/22, Lancet (London, England) 381 (9869) (2013) 836–844, https://doi.org/10.1016/s0140-6736(12)61765-6. PubMed PMID: 23332165.

[6] R. Waksman, F. Prati, N. Bruining, M. Haude, D. Böse, H. Kitabata, P. Erne, S. Verheye, H. Degen, P. Vermeersch, L. Di Vito, J. Koolen, R. Erbel, Serial observation of drug-eluting absorbable metal scaffold: multi-imaging modality assessment, Epub 2013/11/21, Circ. Cardiovasc. Intervent. 6 (6) (2013) 644–653, https://doi.org/10.1161/circinterventions.113.000693. PubMed PMID: 24254708.

[7] M. Haude, H. Ince, A. Abizaid, R. Toelg, P.A. Lemos, C. von Birgelen, E. H. Christiansen, W. Wijns, F.J. Neumann, C. Kaiser, E. Eeckhout, S.T. Lim, J. Escaned, H.M. Garcia-Garcia, R. Waksman, Safety and performance of the second-generation drug-eluting absorbable metal scaffold in patients with de-novo coronary artery lesions (BIOSOLVE-II): 6 month results of a prospective, multicentre, non-randomised, first-in-man trial, Epub 2015/10/17, Lancet (London, England) 387 (10013) (2016) 31–39, https://doi.org/10.1016/s0140-6736(15)00447-x. PubMed PMID: 26470647.

[8] Y. Ueki, L. Räber, T. Otsuka, H. Rai, S. Losdat, S. Windecker, H.M. Garcia-Garcia, U. Landmesser, J. Koolen, R. Byrne, M. Haude, M. Joner, Mechanism of drug-eluting absorbable metal scaffold restenosis: a serial optical coherence tomography study, Epub 2020/02/26, Circ. Cardiovasc. Intervent. 13 (3) (2020) e008657, https://doi.org/10.1161/circinterventions.119.008657. PubMed PMID: 32093514.

[9] C.O. Fallesen, L. Antonsen, A. Maehara, M. Noori, M. Hougaard, K.N. Hansen, J. Ellert, O. Ahlehoff, K.T. Veien, J.F. Lassen, A.B. Junker, H.S. Hansen, L. O. Jensen, Optical coherence tomography- versus angiography-guided magnesium bioresorbable scaffold implantation in NSTEMI patients, Epub 2021/12/25, Cardiovasc. Revascularization Med. : Mol. Interv. 40 (2022) 101–110, https://doi.org/10.1016/j.carrev.2021.12.003. PubMed PMID: 34949544.

[10] K. Song, Y. Bi, H. Zhao, T. Wu, F. Xu, G. Zhao, Structural optimization and finite element analysis of poly-l-lactide acid coronary stent with improved radial strength and acute recoil rate, Epub 2020/03/11, J. Biomed. Mater. Res. B Appl. Biomater. 108 (7) (2020) 2754–2764, https://doi.org/10.1002/jbm.b.34605. PubMed PMID: 32154984.

[11] T. Miyazaki, A. Latib, N. Ruparelia, H. Kawamoto, K. Sato, F. Figini, A. Colombo, The use of a scoring balloon for optimal lesion preparation prior to bioresorbable scaffold implantation: a comparison with conventional balloon predilatation, Epub 2016/04/09, EuroIntervention: J. EuroPCR Coll. Working Group Intervent. Cardiol. Europ. Soc. Cardiol. 11 (14) (2016) e1580–e1588, https://doi.org/10.4244/eijv11i14a308. PubMed PMID: 27056118.

[12] F. Prati, G. Guagliumi, G.S. Mintz, M. Costa, E. Regar, T. Akasaka, P. Barlis, G. J. Tearney, I.K. Jang, E. Arbustini, H.G. Bezerra, Y. Ozaki, N. Bruining, D. Dudek, M. Radu, A. Erglis, P. Motreff, F. Alfonso, K. Toutouzas, N. Gonzalo, C. Tamburino, T. Adriaenssens, F. Pinto, P.W. Serruys, C. Di Mario, Expert review document part 2: methodology, terminology and clinical applications of optical coherence tomography for the assessment of interventional procedures, Epub 2012/06/02, Eur. Heart J. 33 (20) (2012) 2513–2520, https://doi.org/10.1093/eurheartj/ehs095. PubMed PMID: 22653335; PMCID: PMC3470836.

[13] G.S. Mintz, S.E. Nissen, W.D. Anderson, S.R. Bailey, R. Erbel, P.J. Fitzgerald, F. J. Pinto, K. Rosenfield, R.J. Siegel, E.M. Tuzcu, P.G. Yock, American college of cardiology clinical expert consensus document on standards for acquisition, measurement and reporting of intravascular ultrasound studies (IVUS). A report of the American college of cardiology task force on clinical expert consensus documents, Epub 2001/04/13, J. Am. Coll. Cardiol. 37 (5) (2001) 1478–1492, https://doi.org/10.1016/s0735-1097(01)01175-5. PubMed PMID: 11300468.

[14] G.J. Tearney, E. Regar, T. Akasaka, T. Adriaenssens, P. Barlis, H.G. Bezerra, B. Bouma, N. Bruining, J.M. Cho, S. Chowdhary, M.A. Costa, R. de Silva, J. Dijkstra, C. Di Mario, D. Dudek, E. Falk, M.D. Feldman, P. Fitzgerald, H. M. Garcia-Garcia, N. Gonzalo, J.F. Granada, G. Guagliumi, N.R. Holm, Y. Honda, F. Ikeno, M. Kawasaki, J. Kochman, L. Koltowski, T. Kubo, T. Kume, H. Kyono, C. C. Lam, G. Lamouche, D.P. Lee, M.B. Leon, A. Maehara, O. Manfrini, G.S. Mintz, K. Mizuno, M.A. Morel, S. Nadkarni, H. Okura, H. Otake, A. Pietrasik, F. Prati, L. Raber, M.D. Radu, J. Rieber, M. Riga, A. Rollins, M. Rosenberg, V. Sirbu, P. W. Serruys, K. Shimada, T. Shinke, J. Shite, E. Siegel, S. Sonoda, M. Suter, S. Takarada, A. Tanaka, M. Terashima, T. Thim, S. Uemura, G.J. Ughi, H.M. van Beusekom, A.F. van der Steen, G.A. van Es, G. van Soest, R. Virmani, S. Waxman, N.J. Weissman, G. Weisz, Consensus standards for acquisition, measurement, and reporting of intravascular optical coherence tomography studies: a report from the International Working Group for Intravascular Optical Coherence Tomography Standardization and Validation, Epub 2012/03/17, J. Am. Coll. Cardiol. 59 (12) (2012) 1058–1072, https://doi.org/10.1016/j.jacc.2011.09.079. PubMed PMID: 22421299.

[15] S. Nakatani, Y. Sotomi, Y. Ishibashi, M.J. Grundeken, H. Tateishi, E. Tenekecioglu, Y. Zeng, P. Suwannasom, E. Regar, M.D. Radu, L. Räber, H. Bezerra, M.A. Costa, P. Fitzgerald, F. Prati, R.A. Costa, J. Dijkstra, T. Kimura, K. Kozuma, K. Tanabe, T. Akasaka, C. Di Mario, P.W. Serruys, Y. Onuma, Comparative analysis method of permanent metallic stents (XIENCE) and bioresorbable poly-L-lactic (PLLA) scaffolds (Absorb) on optical coherence tomography at baseline and follow-up, Epub 2015/10/09, EuroIntervention: J. EuroPCR Coll. Working Group Intervent. Cardiol. Europ. Soc. Cardiol. 12 (12) (2016) 1498–1509, https://doi.org/10.4244/eijy15m10_03. PubMed PMID: 26448577.

[16] A. Abizaid, R.A. Costa, J. Schofer, J. Ormiston, M. Maeng, B. Witzenbichler, R. V. Botelho, J.R. Costa Jr., D. Chamié, A.S. Abizaid, J.P. Castro, L. Morrison, S. Toyloy, V. Bhat, J. Yan, S. Verheye, Serial multimodality imaging and 2-year clinical outcomes of the novel DESolve novolimus-eluting bioresorbable coronary scaffold system for the treatment of single de novo coronary lesions, Epub 2016/03/26, JACC Cardiovasc. Interv. 9 (6) (2016) 565–574, https://doi.org/10.1016/j.jcin.2015.12.004. PubMed PMID: 27013155.

[17] M. Sabaté, S. Windecker, A. Iñiguez, L. Okkels-Jensen, A. Cequier, S. Brugaletta, S. H. Hofma, L. Räber, E.H. Christiansen, M. Suttorp, T. Pilgrim, G. Anne van Es, Y. Sotomi, H.M. García-García, Y. Onuma, P.W. Serruys, Everolimus-eluting bioresorbable stent vs. durable polymer everolimus-eluting metallic stent in patients with ST-segment elevation myocardial infarction: results of the randomized ABSORB ST-segment elevation myocardial infarction-TROFI II trial, Epub 2015/09/26, Eur. Heart J. 37 (3) (2016) 229–240, https://doi.org/10.1093/eurheartj/ehv500. PubMed PMID: 26405232; PMCID: PMC4712350.

[18] J.K. Simonsen, E.N. Holck, D. Carrie, N. Frey, M. Lutz, J. Weber-Albers, D. Dudek, B. Chevalier, J. Daemen, J. Dijkstra, C. Fox Maule, O. Neghabat, J.F. Lassen, J. Anderson, E.H. Christiansen, A. Abizaid, N.R. Holm, Mechanical performance and healing patterns of the novel sirolimus-eluting bioresorbable Fantom scaffold: 6-month and 9-month follow-up by optical coherence tomography in the FANTOM II study, Epub 2019/04/19, Open heart 6 (1) (2019) e000941, https://doi.org/10.1136/openhrt-2018-000941. PubMed PMID: 30997130; PMCID: PMC6443130.

[19] S. Verheye, J.A. Ormiston, J. Stewart, M. Webster, E. Sanidas, R. Costa, J. R. Costa Jr., D. Chamie, A.S. Abizaid, I. Pinto, L. Morrison, S. Toyloy, V. Bhat, J. Yan, A. Abizaid, A next-generation bioresorbable coronary scaffold system: from bench to first clinical evaluation: 6- and 12-month clinical and multimodality imaging results, Epub 2013/10/22, JACC Cardiovasc. Interv. 7 (1) (2014) 89–99, https://doi.org/10.1016/j.jcin.2013.07.007. PubMed PMID: 24139932.

[20] P.W. Serruys, B. Chevalier, D. Dudek, A. Cequier, D. Carrié, A. Iniguez, M. Dominici, R.J. van der Schaaf, M. Haude, L. Wasungu, S. Veldhof, L. Peng, P. Staehr, M.J. Grundeken, Y. Ishibashi, H.M. Garcia-Garcia, Y. Onuma, A bioresorbable everolimus-eluting scaffold versus a metallic everolimus-eluting stent for ischaemic heart disease caused by de-novo native coronary artery lesions (ABSORB II): an interim 1-year analysis of clinical and procedural secondary outcomes from a randomised controlled trial, Epub 2014/09/19, Lancet (London, England) 385 (9962) (2015) 43–54, https://doi.org/10.1016/s0140-6736(14)61455-0. PubMed PMID: 25230593.

[21] J.L. Gutiérrez-Chico, C. Cortés, M. Schincariol, U. Limon, M. Yalcinli, M.A. Durán-Cortés, M. Jaguszewski, Implantation of bioresorbable scaffolds under guidance of optical coherence tomography: feasibility and pilot clinical results of a systematic protocol, Epub 2018/05/19, Cardiol. J. 25 (4) (2018) 443–458, https://doi.org/10.5603/CJ.a2018.0055. PubMed PMID: 29774520.

[22] D. Kandzari, S. Hearne, G. Kumar, R. Sachdeva, G. Adams, B. Blossom, T. Dahle, K. Sanghvi, M.G. Cohen, G. Imperi, R. Riley, A.P. Almonacid, Procedural effectiveness with a focused force scoring angioplasty catheter: procedural and clinical outcomes from the scoreflex NC trial, Epub 2021/03/31, Cardiovasc. Revascularization Med. : Mol. Interv. 35 (2022) 85–90, https://doi.org/10.1016/j.carrev.2021.03.013. PubMed PMID: 33781677.

[23] A. Maehara, M. Matsumura, Z.A. Ali, G.S. Mintz, G.W. Stone, IVUS-guided versus OCT-guided coronary stent implantation: a critical appraisal, Epub 2017/12/09, JACC Cardiovasc. Imag. 10 (12) (2017) 1487–1503, https://doi.org/10.1016/j.jcmg.2017.09.008. PubMed PMID: 29216976.

[24] P.W. Serruys, Y. Onuma, J.A. Ormiston, B. de Bruyne, E. Regar, D. Dudek, L. Thuesen, P.C. Smits, B. Chevalier, D. McClean, J. Koolen, S. Windecker, R. Whitbourn, I. Meredith, C. Dorange, S. Veldhof, K. Miquel-Hebert, R. Rapoza, H. M. García-García, Evaluation of the second generation of a bioresorbable everolimus drug-eluting vascular scaffold for treatment of de novo coronary artery stenosis: six-month clinical and imaging outcomes, Epub 2010/11/26, Circulation 122 (22) (2010) 2301–2312, https://doi.org/10.1161/circulationaha.110.970772. PubMed PMID: 21098436.

[25] P.W. Serruys, H.M. Garcia-Garcia, Y. Onuma, From metallic cages to transient bioresorbable scaffolds: change in paradigm of coronary revascularization in the upcoming decade?, Epub 2011/11/02, Eur. Heart J. 33 (1) (2012) 16–25b, https://doi.org/10.1093/eurheartj/ehr384. PubMed PMID: 22041548.

[26] S. Brugaletta, J.H. Heo, H.M. Garcia-Garcia, V. Farooq, R.J. van Geuns, B. de Bruyne, D. Dudek, P.C. Smits, J. Koolen, D. McClean, C. Dorange, S. Veldhof, R. Rapoza, Y. Onuma, N. Bruining, J.A. Ormiston, P.W. Serruys, Endothelial-dependent vasomotion in a coronary segment treated by ABSORB everolimus-eluting bioresorbable vascular scaffold system is related to plaque composition at the time of bioresorption of the polymer: indirect finding of vascular reparative therapy?, Epub 2012/04/18, Eur. Heart J. 33 (11) (2012) 1325–1333, https://doi.org/10.1093/eurheartj/ehr466. PubMed PMID: 22507972.

[27] D.J. Kereiakes, S.G. Ellis, C. Metzger, R.P. Caputo, D.G. Rizik, P.S. Teirstein, M. R. Litt, A. Kini, A. Kabour, S.O. Marx, J.J. Popma, R. McGreevy, Z. Zhang, C. Simonton, G.W. Stone, 3-Year clinical outcomes with everolimus-eluting bioresorbable coronary scaffolds: the ABSORB III trial, Epub 2017/11/05, J. Am. Coll. Cardiol. 70 (23) (2017) 2852–2862, https://doi.org/10.1016/j.jacc.2017.10.010. PubMed PMID: 29100702.

[28] P.W. Serruys, B. Chevalier, Y. Sotomi, A. Cequier, D. Carrié, J.J. Piek, A.J. Van Boven, M. Dominici, D. Dudek, D. McClean, S. Helqvist, M. Haude, S. Reith, M. de Sousa Almeida, G. Campo, A. Iñiguez, M. Sabaté, S. Windecker, Y. Onuma, Comparison of an everolimus-eluting bioresorbable scaffold with an everolimus-eluting metallic stent for the treatment of coronary artery stenosis (ABSORB II): a 3 year, randomised, controlled, single-blind, multicentre clinical trial, Epub 2016/11/04, Lancet (London, England) 388 (10059) (2016) 2479–2491, https://doi.org/10.1016/s0140-6736(16)32050-5. PubMed PMID: 27806897.

[29] N. Azzi, W. Shatila, Update on coronary artery bioresorbable vascular scaffolds in percutaneous coronary revascularization, Epub 2021/04/02, Rev. Cardiovasc. Med. 22 (1) (2021) 137–145, https://doi.org/10.31083/j.rcm.2021.01.225. PubMed PMID: 33792255.

[30] T. Barkholt, B. Webber, N.R. Holm, J.A. Ormiston, Mechanical properties of the drug-eluting bioresorbable magnesium scaffold compared with polymeric scaffolds and a permanent metallic drug-eluting stent. Catheterization and cardiovascular interventions, E674-e82. Epub 2019/11/12, Off. J. Soc. Card. Angiogr. Intervent. 96 (7) (2020), https://doi.org/10.1002/ccd.28545. PubMed PMID: 31710149; PMCID: PMC7754471.

[31] M. Haude, H. Ince, R. Toelg, P.A. Lemos, C. von Birgelen, E.H. Christiansen, W. Wijns, F.J. Neumann, E. Eeckhout, H.M. Garcia-Garcia, R. Waksman, Safety and performance of the second-generation drug-eluting absorbable metal scaffold (DREAMS 2G) in patients with de novo coronary lesions: three-year clinical results and angiographic findings of the BIOSOLVE-II first-in-man trial, Epub 2019/02/26, EuroIntervention: J. EuroPCR Coll. Working Group Intervent. Cardiol. Europ. Soc. Cardiol. 15 (15) (2020) e1375–e1382, https://doi.org/10.4244/eij-d-18-01000. PubMed PMID: 30803936.

[32] Y. Ozaki, H.M. Garcia-Garcia, A. Hideo-Kajita, K.O. Kuku, M. Haude, H. Ince, A. Abizaid, R. Tölg, P.A. Lemos, C. von Birgelen, E.H. Christiansen, W. Wijns, J. Escaned, J. Dijkstra, R. Waksman, Impact of procedural characteristics on coronary vessel wall healing following implantation of second-generation drug-eluting absorbable metal scaffold in patients with de novo coronary artery lesions: an optical coherence tomography analysis, Epub 2018/12/28, Europ. Heart J. Cardiovasc. Imag. 20 (8) (2019) 916–924, https://doi.org/10.1093/ehjci/jey210. PubMed PMID: 30590578.

[33] H.M. Garcia-Garcia, M. Haude, K. Kuku, A. Hideo-Kajita, H. Ince, A. Abizaid, R. Tölg, P.A. Lemos, C. von Birgelen, E.H. Christiansen, W. Wijns, J. Escaned, J. Dijkstra, R. Waksman, In vivo serial invasive imaging of the second-generation drug-eluting absorbable metal scaffold (Magmaris - DREAMS 2G) in de novo coronary lesions: insights from the BIOSOLVE-II First-In-Man Trial, Epub 2018/01/03, Int. J. Cardiol. 255 (2018) 22–28, https://doi.org/10.1016/j.ijcard.2017.12.053. PubMed PMID: 29292064.

[34] P. Rola, A. Włodarczak, M. Barycki, M. Szudrowicz, M. Łanocha, J.J. Kulczycki, K. Turkiewicz, K. Woźnica, M. Lesiak, A. Doroszko, Biodegradable polymer DES (ultimaster) vs. Magnesium bioresorbable scaffold (BRS Magmaris) in diabetic population with NSTE-ACS: a one-year clinical outcome of two sirolimus-eluting stents, Epub 2021/12/04, J. Diabetes Res. 2021 (2021) 8636050, https://doi.org/10.1155/2021/8636050. PubMed PMID: 34859105; PMCID: PMC8632392 publication of this paper.

[35] M. Bossard, M. Madanchi, D. Avdijaj, A. Attinger-Toller, G.M. Cioffi, T. Seiler, G. Tersalvi, R. Kobza, G. Schüpfer, F. Cuculi, Long-term outcomes after implantation of magnesium-based bioresorbable scaffolds-insights from an all-comer registry, Epub 2022/05/03, Front Cardiovasc. Med. 9 (2022) 856930, https://doi.org/10.3389/fcvm.2022.856930. PubMed PMID: 35498044; PMCID: PMC9046914.

[36] M. Haude, H. Ince, S. Kische, A. Abizaid, R. Tölg, P. Alves Lemos, N.M. Van Mieghem, S. Verheye, C. von Birgelen, E.H. Christiansen, E. Barbato, H.M. Garcia-Garcia, R. Waksman, Safety and clinical performance of a drug eluting absorbable metal scaffold in the treatment of subjects with de novo lesions in native coronary arteries: pooled 12-month outcomes of BIOSOLVE-II and BIOSOLVE-III. Catheterization and cardiovascular interventions, E502-e11. Epub 2018/08/07, Off. J. Soc. Card. Angiogr. Intervent. 92 (7) (2018), https://doi.org/10.1002/ccd.27680. PubMed PMID: 30079472; PMCID: PMC6586164.

[37] S. Verheye, A. Wlodarczak, P. Montorsi, J. Torzewski, J. Bennett, M. Haude, G. Starmer, T. Buck, M. Wiemer, A.A.B. Nuruddin, B.P. Yan, M.K. Lee, BIOSOLVE-IV-registry: safety and performance of the Magmaris scaffold: 12-month outcomes of the first cohort of 1,075 patients. Catheterization and cardiovascular interventions, Epub 2020/09/04, Off. J. Soc. Card. Angiogr. Intervent. 98 (1) (2021) E1–e8, https://doi.org/10.1002/ccd.29260. PubMed PMID: 32881396; PMCID: PMC8359313.

[38] M. Haude, R. Toelg, P.A. Lemos, E.H. Christiansen, A. Abizaid, C. von Birgelen, F. J. Neumann, W. Wijns, H. Ince, C. Kaiser, S.T. Lim, J. Escaned, E. Eeckhout, H. M. Garcia-Garcia, R. Waksman, Sustained safety and performance of a second-generation sirolimus-eluting absorbable metal scaffold: long-term data of the BIOSOLVE-II first-in-man trial at 5 years, Epub 2021/08/09, Cardiovasc. Revascularization Med. : Mol. Interv. 38 (2022) 106–110, https://doi.org/10.1016/j.carrev.2021.07.017. PubMed PMID: 34364807.

[39] M. Sabaté, F. Alfonso, A. Cequier, S. Romaní, P. Bordes, A. Serra, A. Iñiguez, P. Salinas, B. García Del Blanco, J. Goicolea, R. Hernández-Antolín, J. Cuesta, J. A. Gómez-Hospital, L. Ortega-Paz, J. Gomez-Lara, S. Brugaletta, Magnesium-based resorbable scaffold versus permanent metallic sirolimus-eluting stent in patients with ST-segment elevation myocardial infarction: the MAGSTEMI randomized clinical trial, Epub 2019/09/26, Circulation 140 (23) (2019) 1904–1916, https://doi.org/10.1161/circulationaha.119.043467. PubMed PMID: 31553204.

[40] L. Ortega-Paz, S. Brugaletta, J. Gomez-Lara, F. Alfonso, A. Cequier, S. Romaní, P. Bordes, A. Serra, A. Iñiguez, P. Salinas, B. García Del Blanco, J. Goicolea, R. Hernández-Antolín, J. Cuesta, J.A. Gómez-Hospital, M. Sabaté, Magnesium-based resorbable scaffold vs permanent metallic sirolimus-eluting stent in patients with ST-segment elevation myocardial infarction: 3-year results of the MAGSTEMI randomised controlled trial, Epub 2022/03/01, EuroIntervention: J. EuroPCR Coll. Working Group Intervent. Cardiol. Europ. Soc. Cardiol. 18 (5) (2022) e389–e396, https://doi.org/10.4244/eij-d-21-00651. PubMed PMID: 35225793.

[41] J. Gomez-Lara, L. Ortega-Paz, S. Brugaletta, J. Cuesta, S. Romaní, A. Serra, P. Salinas, B. García Del Blanco, J. Goicolea, R. Hernandez-Antolín, P. Antuña, R. Romaguera, A. Regueiro, F. Rivero, À. Cequier, F. Alfonso, J.A. Gómez-Hospital,

M. Sabaté, Bioresorbable scaffolds versus permanent sirolimus-eluting stents in patients with ST-segment elevation myocardial infarction: vascular healing outcomes from the MAGSTEMI trial, Epub 2020/04/21, EuroIntervention: J. EuroPCR Coll. Working Group Intervent. Cardiol. Europ. Soc. Cardiol. 16 (11) (2020) e913–e921, https://doi.org/10.4244/eij-d-20-00198. PubMed PMID: 32310130.

[42] A. Abizaid, D. Carrié, N. Frey, M. Lutz, J. Weber-Albers, D. Dudek, B. Chevalier, S. C. Weng, R.A. Costa, J. Anderson, G.W. Stone, 6-Month clinical and angiographic outcomes of a novel radiopaque sirolimus-eluting bioresorbable vascular scaffold: the FANTOM II study, Epub 2017/09/25, JACC Cardiovasc. Interv. 10 (18) (2017) 1832–1838, https://doi.org/10.1016/j.jcin.2017.07.033. PubMed PMID: 28935075.

[43] A. Gutiérrez-Barrios, L.L. Gheorghe, S. Camacho Freire, E. Silva, A. Gómez Menchero, M.P. Francisco Jose, D. Cañadas Pruaño, U. Martínez Capoccioni, J. Gomez Lara, T. Bretones Del Pino, G. Calle Perez, Long-term clinical, angiographic, and optical coherence tomography findings of Mg-based bioresorbable scaffold in patients with acute coronary syndrome. Catheterization and cardiovascular interventions, Epub 2021/02/19, Off. J. Soc. Card. Angiogr. Intervent. 98 (1) (2021) E69–e77, https://doi.org/10.1002/ccd.29557. PubMed PMID: 33600069.